LETTER TO THE EDITOR

In situ electronic transport measurement as a tool for investigating the 2D doping in metal–C$_{60}$ interfacial systems

W B Zhao†, J Chen†, K Wu†, J L Zhang†, C Y Li†, D L Yin†, Z N Gu‡, X H Zhou‡ and Z X Jin‡

† Department of Physics, Peking University, Beijing 100871, People's Republic of China
‡ Department of Chemistry, Peking University, Beijing 100871, People's Republic of China

Abstract. The two-dimensional doping by charge transfer and/or diffusion of metal atoms into C$_{60}$ has been studied by *in situ* electronic transport measurements during the deposition of metal–C$_{60}$ ultrathin bilayers. The results show that the transport properties of these interfacial systems are significantly altered by such doping processes. Some useful information about the charge transfer from metal to C$_{60}$ and the electronic transport properties of the metal-doped-monolayer C$_{60}$ can be obtained after careful analysis.

The large interstices in solid C$_{60}$ give opportunities to dope with various kinds of metal atom. However, unlike intercalated graphite, it has been found that only alkali metals [1], alkali earth metals [2] and some rare earth metals [3] can be reacted with C$_{60}$ to form three-dimensional (3D) (bulk) intercalation compounds. It is believed that the dominant factors concerning the possibility of the formation of 3D compounds are the work function ϕ and the cohesive energy E_{coh} of the metal [4]. If the sum of $e\phi$ and E_{coh} is less than the C$_{60}$ LUMO energy E_{LUMO}, the intercalation energy E_{intc} (= $E_{LUMO} - e\phi - E_{coh}$) is positive and the formation of 3D compounds is favoured. The calculation showed that E_{intc} is positive only for the above three sorts of metal, except for Hg. Nevertheless, the two-dimensional (2D) doping by charge transfer and/or diffusion of metal atoms into C$_{60}$ cannot be ruled out. On some metal surfaces overcoated with a C$_{60}$ monolayer, charge transfer and the formation of a metallic interfacial layer have been observed by photoemission spectroscopy [5–7], surface enhanced Raman spectroscopy [7] and STM [8]. Such 2D doping is expected to alter the transport properties of the metal–C$_{60}$ interfacial systems. To this end, we studied several selected metal–C$_{60}$ ultrathin bilayers by means of *in situ* electronic transport measurements.

The fullerenes were formed by a conventional AC arc method, and purified by repeated chromatography until the parity of C$_{60}$ was better than 99.8%. The deposition of metal–C$_{60}$ bilayers was completed using a Balzers UMS-500 UHV system. After thorough degassing, deposition could be carried out at pressures below 1×10^{-6} Pa. The operating pressure was about 1×10^{-7} Pa. Newly cleaved NaCl and mica were used as substrates (1 cm × 0.5 cm). Prior to evaporation, four contacts (gap ∼ 1 mm) for electrical resistance measurements were made by depositing Ag, and connecting Cu wires with silver paint. During the evaporation process, the substrates were kept at room temperature, and the resistance measured *in situ* by an in-line four-probe method. The average film thickness and the deposition rate (∼ 1 nm min^{-1}) were monitored by the quartz oscillation device. We deposit metals as the first
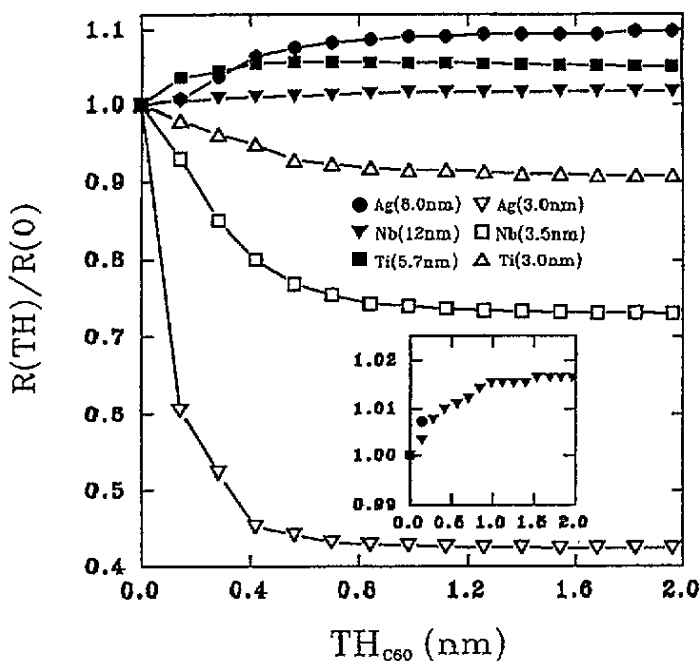
Figure 1. Resistance variation during the C_{60} deposition on Ag, Nb and Ti layers with different thicknesses. The inset shows the detailed resistance increase while adding C_{60} to the more continuous Nb films in an enlarged scale.

layer with different nominal thicknesses from several monolayers to around 10 nm, then add C_{60} to them. In the mean time, the sample resistance was measured *in situ*.

Evidence of charge transfer and surface enhanced scattering effect. Figure 1 shows the resistance change when adding C_{60} to the Ag, Nb and Ti layers with different thicknesses. When depositing C_{60} on an extremely thin discontinuous metal layer, the resistance decreases significantly. However, with increasing metal thickness, i.e., continuity of the metal layers, there is a change in sign of the resistance variation resulting from C_{60} deposition. To obtain further knowledge about the continuity and the conduction mechanism of the metal layers, we measured the resistance–temperature dependence from room temperature down to liquid nitrogen temperature, immediately after the deposition of C_{60} in an ultra-high-vacuum chamber, as can be seen from figure 2. We find that there is a close relationship between the sign of the resistance change when adding C_{60} to the precursor metal films and the temperature coefficient of resistance (TCR). If we denote the resistance change

$$\Delta R \equiv R_f - R_0 \tag{1}$$

where R_0 is the resistance of the precursor metal films and R_f is the final resistance after the C_{60} deposition, then ΔR changes from negative to positive as the TCR of the films changes from negative to positive. Another interesting feature of the measurements is that the resistance variation during C_{60} deposition is mainly restricted within one monolayer of C_{60} (~0.8 nm thick), which indicates that the interaction between metal and C_{60} is limited in such 2D areas.

Because pure C_{60} is insulating (with a conductivity less than 10^{-5} S cm^{-1} [9]), it is reasonable to believe that the resistance change when adding C_{60} onto metal layers is the direct result of metal–C_{60} interaction.
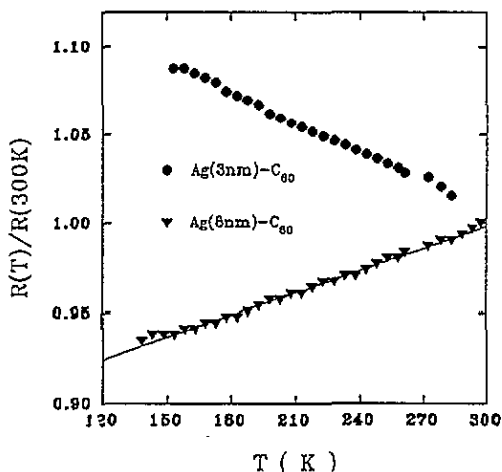
Figure 2. Temperature versus resistance curves for a relatively thick metallic and an ultrathin insulating silver layer after C_{60} deposition.

When the metal layer is around the percolation threshold (TCR < 0), thermally activated electron tunnelling is the main conduction process [10]. Before the deposition of C_{60}, the electrons can only tunnel via the insulating substrate and the vacuum from one isolated metal island to another. When C_{60} is added to the metal films, the involvement of C_{60} as a new channel for electron tunnelling can contribute to the sample resistance drop.

As the metal layer is thick enough to ensure ohmic electron conduction (i.e. the metal clusters have connected with each other to form a continuous conduction network and the film has a positive TCR), we can safely employ the classical resistivity formula as an approximation

$$\rho = \frac{2m}{ne^2\tau} = \frac{2mv}{ne^2} \tag{2}$$

where n denotes the charge density of the metal, m denotes the mass of the electron, τ denotes the average relaxation time and v the scattering frequency. After C_{60} deposition, both n and v may change, therefore resulting in the resistance change

$$\Delta R/R = \delta\rho/\rho = -\delta n/n + \delta v/v. \tag{3}$$

Because the metal–C_{60} interaction is limited to one monolayer of C_{60}, we suppose that metal films donate electrons only to the neighbouring monolayer of C_{60}. For the same kind of metal, the total number of lost electrons is decided by the nature of the bonding between the metal and the monolayer C_{60}, therefore

$$- \delta n/n = \delta N_e/(nd) \tag{4}$$

where δN_e denotes the surface density of electrons donated to C_{60} and d represents the average thickness of the metal films. Supposing the t_{1u} band of C_{60} is filled with six electrons per C_{60} molecule, then $\delta N_e = 6.66 \times 10^{14}$ electrons cm^{-2} (the density of a close-packed (111) monolayer of C_{60} molecules is 1.11×10^{14} molecules cm^{-2}). For a silver film with charge density of 5.86×10^{22} cm^{-3} (bulk value, the effective density in ultrathin films is somewhat smaller than this, usually half the bulk value at most [11]) and thickness of 10 nm, the resistance change due to electron transfer can be of the order of 1% ($\sim$2% after considering the charge density decrease due to the size effect). The contribution of the charge transfer effect should result in an inverse relation between reduced resistance change $\Delta R/R$ and average metal film thickness d.

Now we discuss the scattering term in (3). Because of the nature of 2D interactions, we believe the deposition of C_{60} can only change the surface scattering frequency of electrons

in metal layer ν_s. That means we can rewrite the scattering term as

$$\delta\nu/\nu = \delta\nu_s/\nu = \delta\nu_s/(\nu_i + \nu_s) \tag{5}$$

where ν_i is the scattering frequency inside the metal film. Here, ν_s is small compared with ν_i because the film is thick enough to show metallic conduction characteristics. If $\delta\nu_s$ is proportional to the actual metal–C_{60} contacting area, then $\delta\nu_s$ should decrease with the increase of the film thickness, in other words, with the increase of the film continuity. Thus, the resistance variation due to the surface scattering frequency change should also be dependent on the metal average thickness d and decrease with the increase of d.
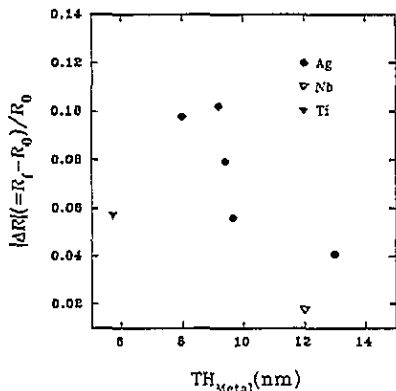

Figure 3. Thickness dependence of the reduced resistance change for metallic Ag, Nb, Ti–C_{60} interfacial systems.

In figure 3, we demonstrate the total resistance change in a reduced scale as a function of precursor metal film thickness for several metallic metal–C_{60} bilayers. It can be seen from the results that $\Delta R/R$ indeed has a tendency to decrease as the metal film thickness increases for Ag–C_{60} systems. The 4–10% increase of the resistance for Ag–C_{60} systems with the precursor silver film thickness ranging from 8 to 13 nm reveals that interaction between silver and C_{60} resulted in a surface enhanced scattering effect on the electron conduction of the silver layer.

Formation of metallic MDML C_{60} (metal-doped-monolayer C_{60})—a possible explanation for the resistance variation in Cu, Cr and Mo–C_{60} systems. The resistance variation as a function of the added C_{60} thickness on the other three kinds of metal, Cu, Cr and Mo films is shown in figure 4. The resistance change behaviour when depositing C_{60} onto the non-metallic (TCR < 0) metal layers is very similar to that in the Ag, Nb and Ti–C_{60} systems, which can be explained as the result of thermally activated electron tunnelling. However, as the metal films approach continuity (TCR > 0), the resistance still drops significantly during the C_{60} depositing process, especially for Cu. This fact suggests the existence of a strong metallic metal-doped-monolayer C_{60} (MDML C_{60}) which may contribute to the resistance decrease in these metal–C_{60} systems. To get more information, we studied the Cu–C_{60} bilayers in more detail. Figure 5 shows the relation of the final resistance and the reduced resistance decrease in different metallic Cu–C_{60} systems. Because the charge density (8.47×10^{22} cm^{-3}) of copper is much higher than that of silver, and the electrons donated to C_{60} cannot be as many as six electrons per C_{60} molecule (the most probable value is three electrons per C_{60}, otherwise the MDML C_{60} may not be metallic), the resistance increase due to this charge transfer effect is less than 1% and can therefore be neglected. If the change of surface scattering can also be neglected compared with the resistance decrease due to the formation of metallic MDML C_{60}, we can estimate the resistivity of this metallic MDML C_{60} as follows
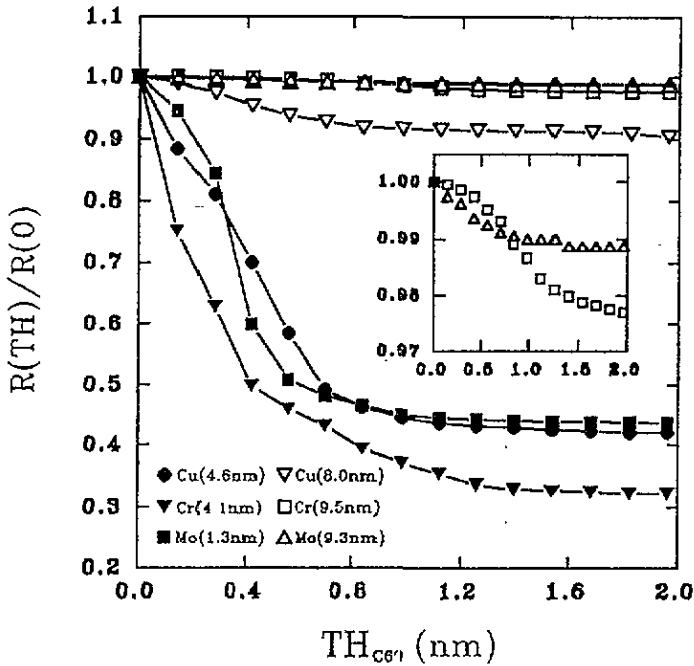
$$1/R_f = 1/R_0 + 1/R_s \tag{6}$$

Figure 4. Resistance change when adding C_{60} to insulating and metallic Cu, Cr and Mo layers. The inset shows the detailed resistance decrease while adding C_{60} on the more continuous metal films (Cr and Mo) in an enlarged scale.

where R_s is the resistance of the MDML C_{60}. The above equation can be rewritten as

$$R_f = R_s |\Delta R| / R_0 \qquad (7)$$

where $|\Delta R| = -\Delta R = R_0 - R_f$. Therefore, the final resistance should have a linear relation with the reduced resistance decrease, and the slope represent the resistance of the MDML C_{60}. From figure 5, we can see the value of R_s is about 3500 Ω. For the one-monolayer-thick (0.8 nm) metal-doped C_{60} with length 1 mm and width 5 mm, the calculation shows the resistivity of the MDML C_{60} is of the order of 2 mΩ cm, which can be compared with that of thick K_3C_{60} films [1]. The detailed data corresponding to figure 5 have been shown in table 1.
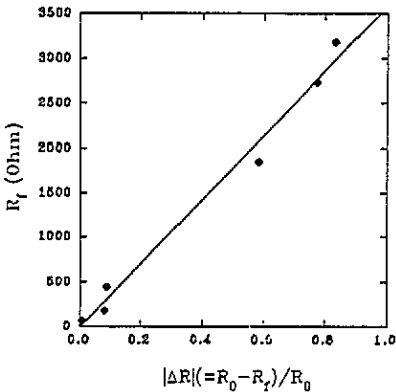

Figure 5. The relationship of the final resistance after C_{60} deposition and the reduced resistance change for Cu–C_{60} bilayers. The slope corresponds to the resistance of the supposed MDML C_{60}. The detailed data are shown in table 1.

Table 1. The detailed data for some Cu–C_{60} bilayer systems which correspond to figure 5.

R_0 (Ω)	R_f (Ω)	Thickness (nm)[a]	$|\Delta R|/R_0$ (%)
62.1	61.7	21.9	0.8
196	180	8.0	8.2
484	441	7.7	8.9
4450	1850	6.3	58.4
12090	2730	5.9	77.4
19300	3180	4.9	83.5

[a] Thickness of the precursor copper films.

The existence of metallic interfacial layer formation in Cu–C_{60} systems has been proved by photoemission spectroscopy study [7]. However, the extraordinarily low resistivity for such a thin layer of MDML C_{60} suggests that other surface factors which favour the resistance decrease of these metal–C_{60} bilayers may also exist, such as the negative interfacial energy between Cu and C_{60} [12].

The electronic transport behaviour of the 2D doping was studied by means of *in situ* resistance measurements during the process of overcoating C_{60} on ultrathin metal layers. The interactions between the selected metal and C_{60} in this letter can be divided into two main kinds by the resistance variation of adding C_{60} to the relatively thick metallic metal layers. For Ag, Nb, Ti, the interfacial bonding with the monolayer of C_{60} may not be metallic or at least is not strongly metallic, therefore the resistance increase due to charge transfer and the surface enhanced scattering effect can easily be seen. For C_{60}–Cu, Cu, Mo systems however, the MDML C_{60} may be strongly metallic and the negative interfacial bonding energy may also exist.

Finally, we want to note that the present work is still semi-quantitative due to the limitations of the sample preparation technique and the scattering of the data. Experiments based on atomically smooth ultrathin epitaxial and polycrystal metal films grown on mica substrates together with high-resolution TEM study are now in progress. We hope a more accurate physical picture of the transport properties of these metal–C_{60} interfacial systems will be given in the near future.

References

[1]   Haddon R C *et al* 1991 *Nature* **350** 320
[2]   Kortan A F *et al* 1992 *Nature* **355** 529
[3]   Ohno T R *et al* 1992 *Phys. Rev.* B **46** 10437
[4]   Wertheim G K *et al* 1993 *Solid State Commun.* **88** 97
[5]   Ohno T R *et al* 1991 *Phys. Rev.* B **44** 13747
[6]   Ohno T R *et al* 1993 *Phys. Rev.* B **47** 2389
[7]   Chase S J *et al* 1992 *Phys. Rev.* B **46** 7873
[8]   Gimzenski J K *et al* 1994 *Phys. Rev. Lett.* **72** 1036
[9]   Palstra T T M *et al* 1992 *Phys. Rev. Lett.* **68** 1054
[10] Abeles B 1975 *Adv. Phys.* **24** 407
[11] Fisher G *et al* 1980 *Phys. Rev.* B **22** 6065
[12] Zhao W B *et al* 1992 *J. Phys.: Condens. Matter* **4** L513